The tumor suppressors *Ink4c* and *p53* collaborate independently with *Patched* to suppress medulloblastoma formation

Tamar Uziel,[1,9] Frederique Zindy,[1,9] Suqing Xie,[1] Youngsoo Lee,[1] Antoine Forget,[1] Susan Magdaleno,[2] Jerold E. Rehg,[3] Christopher Calabrese,[2] David Solecki,[7] Charles G. Eberhart,[6] Sarah E. Sherr,[4] Sarah Plimmer,[8] Steven C. Clifford,[8] Mary E. Hatten,[7] Peter J. McKinnon,[1] Richard J. Gilbertson,[2] Tom Curran,[2] Charles J. Sherr,[1,5] and Martine F. Roussel[1,10]

Departments of [1]Tumor Cell Biology and Genetics, [2]Developmental Neurobiology, [3]Pathology, [4]Hematology-Oncology, and [5]Howard Hughes Medical Institute at St. Jude Children's Research Hospital, Memphis, Tennessee 38105, USA; [6]Department of Pathology, Johns Hopkins University, Baltimore, Maryland 21205, USA; [7]Laboratory of Developmental Neurobiology, Rockefeller University, New York, New York 10021, USA; [8]Northern Institute for Cancer Research, University of Newcastle, Newcastle-upon-Tyne NE2 4HH, United Kingdom

Recurrent genetic alterations in human medulloblastoma (MB) include mutations in the sonic hedgehog (SHH) signaling pathway and *TP53* inactivation (~25% and 10% of cases, respectively). However, mouse models of MB, regardless of their initiating lesions, generally depend upon *p53* inactivation for rapid onset and high penetrance. The gene encoding the cyclin-dependent kinase inhibitor $p18^{Ink4c}$ is transiently expressed in mouse cerebellar granule neuronal precursor cells (GNPs) as they exit the cell division cycle and differentiate. Coinactivation of *Ink4c* and *p53* provided cultured GNPs with an additive proliferative advantage, either in the presence or absence of Shh, and induced MB with low penetrance but with greatly increased incidence following postnatal irradiation. In contrast, mice lacking one or two functional *Ink4c* alleles and one copy of *Patched* (*Ptc1*) encoding the Shh receptor rapidly developed MBs that retained wild-type *p53*. In tumor cells purified from double heterozygotes, the wild-type *Ptc1* allele, but not *Ink4c*, was inactivated. Therefore, when combined with *Ptc1* mutation, *Ink4c* is haploinsufficient for tumor suppression. Methylation of *INK4C* (*CDKN2C*) was observed in four of 23 human MBs, and $p18^{INK4C}$ protein expression was extinguished in 14 of 73 cases. Hence, $p18^{INK4C}$ loss may contribute to MB formation in children.

[*Keywords*: Cyclin-dependent kinase inhibitors; haploinsufficiency; sonic hedgehog signaling]

Supplemental material is available at http://www.genesdev.org.

Received May 31, 2005; revised version accepted September 9, 2005.

Neuronal proliferation, differentiation, and migration are coordinated during cerebellar development, and disruption of these processes can lead to medulloblastoma (MB), the most common malignant pediatric brain tumor (Gilbertson 2004; Marino 2005). Unlike most organogenesis, the cerebellum is largely formed after birth. In the newborn mouse (postnatal day 0 [P0]), the cerebellum is only composed of a thin layer of granule neuronal precursor cells (GNPs) overlying the Purkinje cell plate. Purkinje neurons produce the mitogen sonic hedgehog (Shh) that drives a massive proliferation of GNPs between P1 and P15, thereby expanding the external germinal layer (EGL). GNPs then exit the cell division cycle, extend axons, and migrate inward through the underlying Purkinje layer to form the more deeply situated internal granule layer (IGL). Differentiation of granule neurons results in the elaboration of parallel fibers within the external molecular layer of the cerebellum and the formation of synapses on the dendritic arbors of Purkinje cells (Goldowitz and Hamre 1998; Wang and Zoghbi 2001; Hatten 2002).

Recurrent genetic alterations in childhood MBs include lesions in components of the SHH and WNT signaling pathways, persistent expression of pro-proliferative cell cycle control genes such as *MYCN*, *cyclin D1*, and *cyclin D2* (*CCND1* and *CCND2*, respectively), and inactivation of the *TP53* tumor suppressor (Gilbertson 2004; Marino 2005). While these molecular alterations might account for the development of certain subgroups of human MB, the genetic changes that contribute to the majority of these tumors are unknown. Mouse models of MB mimic different subsets of the human tumors

[9]These authors contributed equally to this work.
[10]Corresponding author.
E-MAIL martine.roussel@stjude.org; FAX (901) 495-2381.
Article published online ahead of print. Article and publication date are at http://www.genesdev.org/cgi/doi/10.1101/gad.1368605.

(Goodrich et al. 1997; Marino et al. 2000; Wetmore et al. 2001; Lee and McKinnon 2002; Tong et al. 2003; Zindy et al. 2003). The patterns of gene expression from both human and mouse MBs much more closely resemble that in the P5 rather than adult mouse cerebellum (Zhao et al. 2002; Lee et al. 2003; Kim et al. 2003; Kho et al. 2004), consistent with the idea that the initiating tumor cells might arise from GNPs.

Cyclin D1, cyclin D2, and N-Myc are essential for cerebellar organogenesis (Ciemerych et al. 2002; Knoepfler et al. 2002) and drive very rapid proliferation of GNPs within the EGL in response to Shh signaling (Kenney and Rowitch 2000; Kenney et al. 2003). This process places a premium on the ability of the cell cycle checkpoint machinery to eliminate cells that have sustained replicative DNA damage, and the cell cycle and DNA damage control machinery act in concert to prevent tumor formation. In the mouse, inactivation of both *Rb* and *p53*, but neither gene alone, in the developing cerebellum results in MB with complete penetrance (Marino et al. 2000). Loss of *p53*, together with either heterozygous deletion of the *Patched* (*Ptc1*) gene encoding the Shh receptor or with complete inactivation of *Ligase IV*, leads to the same outcome (Wetmore et al. 2001; Lee and McKinnon 2002). Disruption of poly (ADP-ribose) polymerase (PARP-1) also causes a high incidence (~50%) of aggressive brain tumors in *p53*-null mice, with typical features of human MB (Tong et al. 2003), again pointing to the importance of DNA damage sensing, repair, and p53 checkpoint control in limiting tumorigenesis. However, *TP53* mutations are relatively rare in human MB, and *RB* mutations have not been reported.

While cell proliferation is driven by cyclin-dependent kinases (CDKs), exit from the cell cycle is regulated in part by CDK inhibitory proteins, only two of which are normally expressed in the EGL (Miyazawa et al. 2000; Zindy et al. 2003). One of these genes, *Ink4c*, encodes a specific inhibitor of cyclin D-dependent kinases, and its mRNA expression is confined to the EGL but is absent in post-mitotic granule neurons (Cunningham and Roussel 2001; Zindy et al. 2003). The other, $p27^{Kip1}$, is an inhibitor of cyclin E- and A-dependent CDKs that is expressed in post-mitotic granule neurons within the inner EGL but, unlike $p18^{Ink4c}$, persists in mature granule neurons within the IGL (Miyazawa et al. 2000). This pattern of expression suggested that $p18^{Ink4c}$ might play some role in "timing" the exit of GNPs from the cell division cycle and their subsequent differentiation within the EGL, whereas $p27^{Kip1}$ might be required for maintaining post-mitotic neurons in a quiescent state (Zindy et al. 1999). Loss of *Kip1*, *Ink4c*, or both in mice does not overtly affect cerebellar development, but the combined inactivation of *Ink4c* and *p53* results in MB with low penetrance. Here, we define a role for *Ink4c* in suppressing medulloblastomas induced by mutations in *p53* or *Ptc1*, demonstrate that combined *Ink4c* and *Ptc1* loss accelerate MB independently of *p53* inactivation, provide evidence that *Ink4c* can function as a haploinsufficient tumor suppressor, and implicate human *INK4C* (*CDKN2C*) in pediatric MB.

Results

Transient Ink4c expression in the EGL

We used in situ hybridization to compare the pattern of *Ink4c* expression in the mouse P7 cerebellum with that of *Math1 (Atoh1)*, which encodes a transcription factor

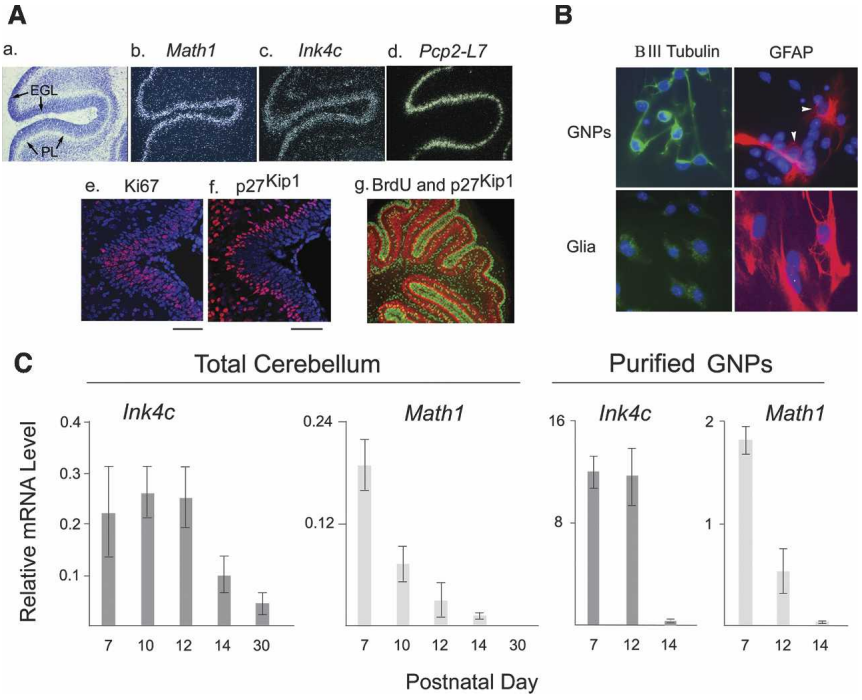

Figure 1. Spatial and temporal expression of *Ink4c* in the developing cerebellum. (*A*) Morphology of the P7 cerebellum (panel *a*) and expression of selected RNAs (panels *b–d*) on serial sections as detected by in situ hybridization with anti-sense probes. The arrows in panel *a* indicate the positions of the Purkinje layer (PL) and EGL. Panels *e–g* illustrate protein expression by immunohistochemistry. Lines *below* denote the EGL. Panel *g* shows double staining for BrdU (green) and $p27^{Kip1}$ (red). (*B*) GNPs and glial cells separated on Percoll gradients were stained for neuronal (βIII tubulin) and glial (GFAP) markers. The white arrows indicate two GFAP-positive cells contaminating the DAPI-stained GNPs. (*C*) Results of quantitative PCR analysis using RNAs extracted at the indicated days (abscissa) and primers directed to *Ink4c* and *Math1*.

expressed in proliferating GNPs (Fig. 1A, panel b), and *Pcp2-L7*, a marker of Purkinje cells (Fig. 1A, panel d). *Ink4c* was expressed within the EGL in a pattern broader than that of *Math1*, but neither of the two genes was expressed within the deeper EGL closer to the underlying Purkinje cell layer (Fig. 1A, cf. panels b,c and d). This pattern of *Ink4c* expression suggested that it is induced in dividing cells and transiently maintained as GNPs exit the cycle and differentiate. Immunostaining of mouse $p18^{Ink4c}$ has not been readily achieved with the antibodies presently available. In contrast, this method is mandatory for studies of $p27^{Kip1}$ expression, which is predominantly regulated post-transcriptionally. In contrast to *Ink4c*, $p27^{Kip1}$ is up-regulated in the premigratory zone of the EGL in Ki67-negative cells that have exited the division cycle (Fig. 1A, panels e,f). Immunofluorescence staining with antibodies to BrdU (green) and to $p27^{Kip1}$ (red) confirmed that this CDK inhibitor is expressed only in post-mitotic cells within the EGL (Fig. 1A, panel g) and maintained within the IGL of the adult brain (Miyazawa et al. 2000).

To study the timing of *Ink4c* expression during the period when cells migrate from the EGL into the IGL, we performed quantitative real-time PCR using RNA extracted from whole cerebella and from purified GNPs isolated from them. Expression of *Ink4c* and *Math1* was concordant at P7, but *Ink4c* expression declined less precipitously than *Math1* and was maintained through P12 (Fig. 1C). Fractionation of explanted cells by gradient centrifugation was then used to separate the denser granule neurons from glial cells (Hatten et al. 1998). Purified cells consisted of >95% GNPs as measured by immunofluorescence with markers for neurons (βIII tubulin) versus glial cells (GFAP) (Fig. 1B). *Ink4c* RNA expression was restricted to GNPs isolated from P7 to P12 but was extinguished thereafter (Fig. 1C) and was less robust in purified fractions containing glia and Purkinje neurons (shown in Fig. 5C, below), consistent with observations that *Ink4c* is not expressed in the IGL (Zindy et al. 2003).

MB in mice doubly deficient for p53 and Ink4c

By 5 mo of age, up to 25% of double knock-out (DKO) mice lacking *Ink4c* and *p53* develop MB, but animals lacking either gene alone do not (Zindy et al. 2003). The protracted time of onset and relatively low incidence of MBs in DKO animals implies that other mutations contribute to their formation. To assess the possibility that consistent chromosomal aberrations might accompany tumor formation, colcemid was administered intraperitoneally to moribund DKO animals that were sacrificed 4 h later, and spectral karyotyping was performed on tumor cell metaphases. In two of two mice studied, the only consistent chromosomal anomaly in tumor cells was the loss of a single copy of chromosome 13 where the *Ptc1* gene resides. Quantitative real-time PCR of RNA extracted from the whole tumor mass revealed that five of seven such tumors expressed the *Ptc1* gene, but no signal was detected in two (data not shown). However, *Math1* expression was readily detected in each tumor. These results suggested that *Ptc1* might be completely inactivated in some of these MBs (see below).

In an attempt to increase the incidence of MB formation, we exposed mice lacking *p53, Ink4c,* or both genes to 4 Gy total body γ-radiation at P5 or P6 when proliferation of GNPs in the EGL is very rapid. Irradiated mice retaining both alleles of *p53*, regardless of their *Ink4c* status, did not develop cerebellar tumors (Table 1). Surprisingly, however, more than two-thirds of irradiated mice lacking *p53* alone developed MBs (Table 1). Because DKO mice simultaneously develop other tumors that limit their lifespan, we engineered *Ink4c*-null mice expressing transgenes encoding Cre recombinase driven either by a Nestin or GFAP promoter, and interbred these with mice containing Cre-excisable ("floxed") $p53^{FL}$ alleles. Exposure of these animals to 19 Gy γ-irradiation at P5 indicated that Nestin-Cre conditionally ablated p53 expression within the EGL (Supplementary Fig. 1A), whereas GFAP-Cre was far less effective (Supplementary Fig. 1B). A lower dose of γ-irradiation (4 Gy) administered at P5 induced MBs in four of four $Ink4c^{-/-}$, Nestin-Cre, $p53^{-/FL}$ mice and in two of five $Ink4c^{+/+}$, Nestin-Cre, $p53^{-/FL}$ animals by 5 mo of age (Table 1). Thus, somatic inactivation of *p53* also predisposes to radiation-induced MB formation. Inactivation of *Ink4c* was not required for tumorigenesis, although there was a trend toward higher penetrance in its absence. Given that MBs have been only rarely observed in unirradiated *p53*-null mice (Donehower et al. 1992; Jacks et al. 1994; Marino et al. 2000), these findings highlight the role of p53 in eliminating GNPs that have sustained DNA damage.

Necropsy of moribund irradiated animals indicated that those lacking *Ink4c* had earlier evidence of tumors characterized by proliferation of neuronal cells within the molecular layer of the cerebellum where MBs characteristically arise (Fig. 2A shows a very early lesion). Because all GNPs normally exit the EGL, some irradiated progenitor cells lacking *p53* and *Ink4c* might have failed to migrate into the IGL. When we sacrificed apparently healthy irradiated mice lacking *Ink4c* alone at 6 mo of age, we invariably detected abnormal microscopic foci of neuronal cells in the cerebellar molecular layer (Fig. 2B), even though these mice did not develop MB (Table 1). These cells expressed the GABA(A) receptor α6 subunit (Fig. 2C), a marker of post-mitotic, differentiated granule neurons that is not detected in GNPs. None of

Table 1. *Incidence of medulloblastomas in* Ink4c, p53 *doubly deficient animals irradiated at P5*

Genotype	Affected/total animals (% incidence)
$Ink4c^{-/-}$, $p53^{+/+}$	0/20 (0%)
$Ink4c^{+/-}$, $p53^{+/-}$	2/10 (20%)
$Ink4c^{+/+}$, $p53^{-/-}$	13/19 (68%)
$Ink4c^{+/-}$, $p53^{-/-}$	15/17 (88%)
$Ink4c^{-/-}$, $p53^{-/-}$	18/24 (75%)
$Ink4c^{-/-}$, $p53^{-/FL}$, Nestin-Cre	4/4 (100%)
$Ink4c^{+/+}$, $p53^{-/FL}$, Nestin-Cre	2/5 (40%)

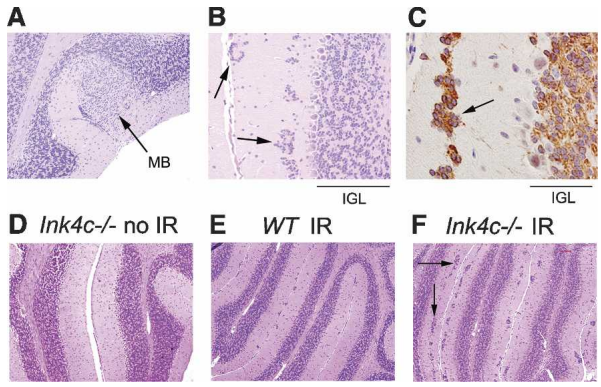

Figure 2. Morphologic analysis of cerebella from *Ink4c*$^{-/-}$ and *Ink4c*$^{-/-}$–*p53*$^{-/-}$ mice. (*A*) An early MB infiltrating the molecular layer of an *Ink4c*$^{-/-}$–*p53*$^{-/-}$ animal irradiated at P5 (100× magnification). (*B*,*C*) Arrows in *B* indicate "nests" of neuronal cells (200× magnification) observed in an overtly healthy *Ink4c*-null mouse at 30 wk of age following irradiation at P5. Staining for GABA(A) receptor α6 subunit in *C* (400×) illustrates the differentiated neuronal origin of similar cellular foci in another animal. Bars *beneath B* and *C* define the position of the IGL. *D–F* illustrate representative sections of cerebella (100× magnification) from an unirradiated *Ink4c*-null mouse (*D*), and from irradiated wild-type (*E*) and *Ink4c*-null (*F*) animals. Arrows in *F* designate representative nests.

these cells stained positively for Ki67, a proliferation marker (data not shown). Possibly, these aberrantly situated nests of noncycling neuronal cells represent the residua of earlier ectopic hyperplastic foci within which *p53* inactivation might provide a more fertile ground for tumorigenesis.

Because irradiation of wild-type mice at P6 can induce a delay in the migration of cells from the EGL followed by their death (Hyodo-Taguchi et al. 1998), we exposed cohorts of wild-type and *Ink4c*-null mice (10 animals per group) to 4 Gy at P6, sacrificed them at P30, and scored cerebellar sections double-blind for the presence of neuronal nests. No such foci were observed in the cerebella of unirradiated animals regardless of their genotype (Fig. 2D), and only few were detected in irradiated wild-type mice, where they generally accumulated at the external surface of the molecular layer (Fig. 2E). In contrast, approximately threefold more neuronal foci, located more deeply within the molecular layer, were observed in all irradiated *Ink4c*-null animals (Fig. 2F). Thus, *Ink4c* loss appears to contribute to the migration defect observed in irradiated mice and enables aberrant foci to persist thereafter (Fig. 2B).

Loss of Ink4c and p53 provides GNPs with an additive proliferative advantage

When *Ink4c-p53* DKO mice were injected with BrdU and their cerebella were fixed in situ by perfusion 9 h later, examination of tissue from mice at 1 mo of age revealed that BrdU-positive cells resided in the superficial molecular layer and in the IGL at a time when virtually all proliferation should have ceased (Supplementary Fig. 2). BrdU-stained cells were counted in representative sections, revealing a threefold increased number in DKO versus wild-type cerebella (191 ± 45 vs. 57 ± 37, respectively). None of the BrdU-positive cells stained with antibodies to GFAP (data not shown). This again suggested that GNPs lacking both *Ink4c* and *p53* fail to properly differentiate and remain in the EGL at a time when neuronal cells should have normally exited.

To address whether loss of *Ink4c* and *p53* affected the proliferation potential of GNPs in the EGL or/and their sensitivity to Shh, we purified them at different times after birth from the cerebella of wild-type and DKO mice and compared their proliferative potential in culture. Cells were isolated at P7, a time at which GNPs exhibit maximal proliferation in the EGL, as well as at P10 and P12, which represent developmental stages at which GNPs normally exit the cell cycle, differentiate, and migrate to the IGL (Goldowitz and Hamre 1998; Wechsler-Reya and Scott 2001). Purified GNPs were pulsed with BrdU for 22 h at different times after plating in the presence or absence of Shh, and BrdU-positive cells visualized by immunofluorescence were counted.

Purified GNPs from wild-type and *Ink4c-p53* DKO cerebella at P7 and P10 proliferated indistinguishably during the first 22 h in culture after plating in the absence of Shh (Fig. 3A). By P12, however, 50% of the wild-type GNPs had lost their capacity to incorporate BrdU as compared with DKO cells (Fig. 3A). Three days after plating in the absence of Shh, most wild-type cells, even when harvested from P7 cerebella, had exited the cell cycle, whereas a significant fraction of DKO cells continued to incorporate BrdU, even when derived at P10 and P12 (Fig. 3B). The observation that only a small fraction of GNPs lacking both *p53* and *Ink4c* remained in cycle after 3 d in culture in the absence of mitogen suggested that, in spite of their proliferative advantage, DKO GNPs remain Shh dependent.

Because differentiated GNPs cannot re-enter the cell cycle when stimulated with Shh (Kenney and Rowitch 2000), we added Shh to the medium 24 h after plating the cells and performed BrdU labeling for a 22-h interval before fixing cells 72 h after plating. For cells harvested at P7, no significant differences were seen in the number of BrdU-positive GNPs obtained from either wild-type or DKO animals (Fig. 3C), similar to what was seen in 1-d cultures lacking Shh (Fig. 3A). However, when GNPs from P10 and P12 mice were evaluated, the number of wild-type cells that incorporated BrdU was significantly less than that in the DKO population (Fig. 3C). Comparison of results obtained with P10 and P12 cells plated without (Fig. 3B) or with (Fig. 3C) Shh underscores the greatly enhanced proliferative response of these cells to the growth factor.

We used the same protocol to compare the responses of GNPs purified from P10 *Ink4c*-null and *p53*-null mice with those from wild-type and DKO littermates (Fig. 3D–F). Again, no differences were observed between P10 cells of different genotypes scored after 1 d in culture in the absence of Shh (Fig. 3D). However, while only few

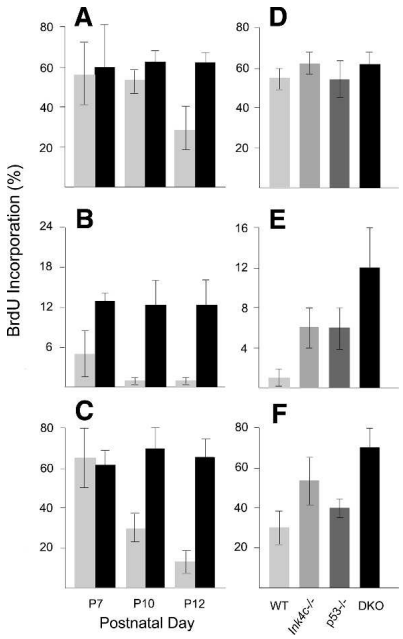

Figure 3. Proliferation potential of cultured GNPs of different *p53* and *Ink4c* genotypes. (*A–C*) Cells purified from mice of the indicated ages (*bottom*) and genotypes (light-gray bars, wild type; black bars, $Ink4c^{-/-}$–$p53^{-/-}$ double null [DKO]) were pulsed with BrdU and stained with anti-BrdU and with DAPI. The percentage of different populations incorporating BrdU is indicated on the ordinate. (*A*) Cells were labeled for 22 h after plating in medium lacking Shh. (*B*) Cells were labeled for 22 h at 46 h after plating in medium lacking Shh. (*C*) Cells were cultured for 1 d in the absence of Shh, after which Shh was added for the next 2 d. Cells were labeled with BrdU during the last 22-h interval. (*D–F*) All experiments were performed with GNPs from P10 cerebella isolated from mice of the genotypes indicated at the *bottom*. Conditions for culture used in *D–F* were identical to those defined for *A–C*, respectively. All differences between genotypes discussed in the text were highly significant (all $p < 0.025$ except for wild type vs. *p53*-null cells at P10 in *F* [$p = 0.08$]).

wild-type cells incorporated BrdU after 3 d of culture in the absence of Shh, a significantly greater fraction of DKO cells remained in cycle (Fig. 3B,E). GNPs lacking either *Ink4c* or *p53* each exhibited half-maximal rates of BrdU incorporation when compared with DKO cells (Fig. 3E). When cells were stimulated with Shh 24 h after plating and were pulsed with BrdU for 22 h between days 2 and 3 of culture, the level of BrdU incorporation in P10 cells lacking either *Ink4c* or *p53* was again lower than that observed in the DKO population (Fig. 3F). Thus, loss of *Ink4c* or *p53* independently extends the temporal window of responsiveness of GNPs to Shh (Fig. 3F), and their coinactivation provides an additive proliferative advantage either in the absence (Fig. 3E) or presence (Fig. 3F) of Shh.

Loss of Ink4c collaborates with Shh signaling in tumorigenesis

Given the loss of one copy of chromosome 13 in MBs arising in mice lacking both *Ink4c* and *p53*, the complete inactivation of *Ptc1* in some of these tumors, and the ability of *Ink4c* loss to contribute independently of *p53* to GNP proliferation, we assessed whether *Ink4c* loss alone could collaborate with *Ptc1* inactivation to enhance the proliferation of GNPs and to accelerate MB formation. *Ptc1* heterozygous mice were interbred to *Ink4c*-null animals to yield $Ptc1^{+/-}$ littermates containing two, one, or no functional *Ink4c* alleles. GNPs isolated from the cerebella of $Ptc1^{+/-}$–$Ink4c^{-/-}$ mice at P10 were plated in culture and pulsed with BrdU. Like cells lacking *Ink4c*, *p53*, or both (Fig. 3D), cells obtained from $Ptc1^{+/-}$ animals, either containing or lacking *Ink4c*, incorporated BrdU with similar efficiency when scored after 1 d in culture in the absence of Shh (Fig. 4, day 1). However, after 3 d in culture without Shh, inactivation of *Ptc1* and *Ink4c* contributed a greater proliferative advantage than loss of *Ptc1* alone, even though p53 function was preserved (see below); as expected, wild-type cells fully differentiated and did not proliferate at all (Fig. 4, day 3).

Although few $Ptc1^{+/-}$–$Ink4c^{+/+}$ mice developed MBs by 40 wk of age, $Ptc1^{+/-}$ mice that lacked one or two *Ink4c* alleles exhibited an earlier onset of MB with a greatly increased incidence (Fig. 5A). Notably, on the $Ptc1^{+/-}$ background, the tumor incidence in $Ink4c^{+/-}$ mice did not differ significantly from that of $Ink4c^{-/-}$ animals, suggesting that *Ink4c* may be haploinsufficient for tumor suppression. MBs from these animals were morphologically similar to tumors arising in $Ptc1^{+/-}$ or $Ink4c^{-/-}$–$p53^{-/-}$ DKO mice (data not shown). FACs analysis of DNA content of uncultured GNPs purified by gradient centrifugation from normal P5 and P10 cerebella and of tumor cells from $Ptc1^{+/-}$–$Ink4c^{+/-}$ mice (two in each group) indicated that the S-phase fraction of MBs (21.4%, 21.5%) closely reflected that of P5 (22%, 23%) as opposed to P10 (12%, 11%) GNPs. Profiling of $Ptc1^{+/-}$–$Ink4c^{+/-}$ or $Ptc1^{+/-}$–$Ink4c^{-/-}$ MBs by use of Affymetrix microchip arrays showed a remarkable consistency of gene expression similar to the patterns realized with MBs arising in other mouse models, including $Ptc1^{+/-}$, $Ptc1^{+/-}$–$p53^{-/-}$, and $Ink4c^{-/-}$–$p53^{-/-}$ animals (Fig. 5B), and their expression signatures again more closely resembled that seen in the P5 cerebellum rather than the adult organ. Genes overexpressed in each of these tumors as

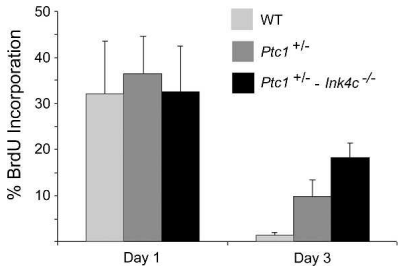

Figure 4. Proliferation of cultured GNPs from $Ptc1^{+/-}$, and $Ptc1^{+/-}$–$Ink4c^{-/-}$ mice. Cells purified from P10 mice were plated and maintained for either 1 or 3 d in the absence of Shh. Cells were pulsed with BrdU for the last 22-h interval prior to fixation and enumeration.

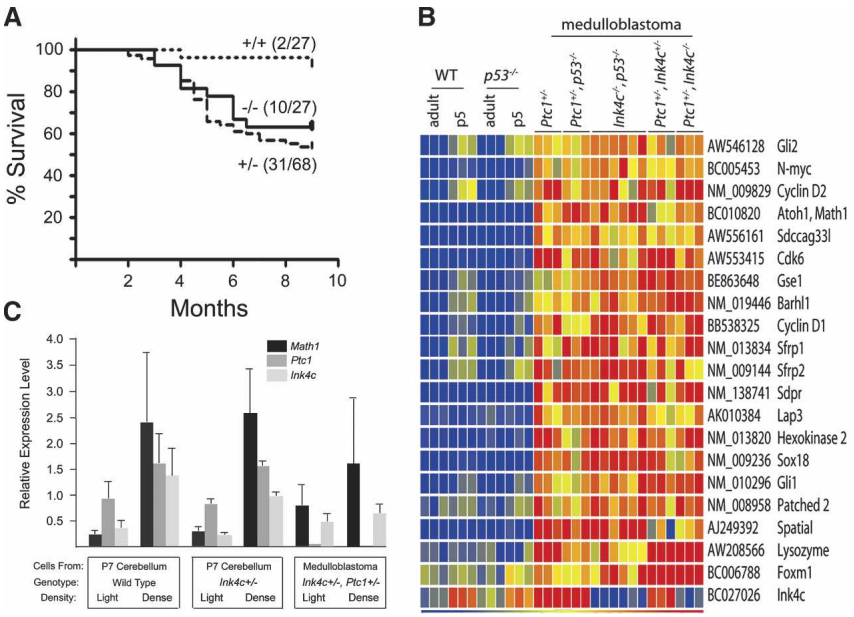

Figure 5. Tumor incidence and gene expression in MB from $Ptc1^{+/-}$, $Ink4c^{+/-}$, and $Ptc1^{+/-}$–$Ink4c^{-/-}$ mice. (*A*) Survival curves of $Ptc1^{+/-}$ mice with the indicated *Ink4c* genotypes. The number of animals with MB versus the total number of mice in each cohort is indicated in parentheses. (*B*) Results of gene profiling using Affymetrix Genechip microarrays. RNAs extracted from P5 and adult cerebella from wild-type or *p53*-null mice, or from medulloblastomas from animals of the indicated genotypes, were evaluated as described (Lee et al. 2003). RNAs from P5 cerebella were compared with those from adult 9-wk-old cerebella, whereas tumor RNAs were compared with those from P5 cerebella. Selected genes from a group of 30 that are all commonly overexpressed in different tumors, regardless of their founding mutations, are shown. *Ink4c* was included in the illustrated set (*bottom* of list). A gradient "heat spectrum" appears at the *bottom* with genes more highly overexpressed noted in red and those least overexpressed indicated in blue. (*C*) Quantitative real-time PCR analysis of *Ptc1* (dark-gray bars) and *Ink4c* (light-gray bars) RNAs extracted from gradient density-fractionated cell populations from normal P7 cerebella and from tumors of the indicated genotypes. *Math 1* (black bars) was used as an internal control.

compared with their levels in cerebella from P5 mice included *Gli*, *Gli2*, *Foxm1* (a Gli target gene), and *Patched-2*, demonstrating up-regulation of the Shh signaling pathway; as expected, *Math1*, *cyclin D1*, *cyclin D2*, and N-*Myc* transcripts were also relatively abundant.

Importantly, *Ink4c* expression was still detected by gene profiling in MBs from *Ink4c* heterozygous mice (Fig. 5B, bottom row). We confirmed these findings by performing RT–PCR with the same RNAs that were used for gene profiling. In three of three tumors from doubly heterozygous animals, *Ink4c* mRNA was expressed, whereas no signal was detected using control RNAs from tumors lacking both *Ink4c* alleles (negative RT–PCR data not shown). Because these analyses did not rigorously demonstrate that *Ink4c* expression was strictly limited to tumor cells, we separated GNP-like tumor cells from the remaining less dense population on Percoll gradients and used quantitative real-time PCR to study both *Ink4c* and *Ptc1* expression (Fig. 5C). In parallel, we again separated cell populations from normal P7 cerebella of both wild-type and *Ink4c* heterozygous animals. *Math1* was used as an internal control, since its expression is limited to proliferating GNPs and GNP-like tumor cells. As expected, *Math1* expression (Fig. 5C, black bars) was enriched in normal GNPs and in tumor cells ("dense" fractions), but not in the remaining cell populations ("light" fractions). While the wild-type *Ptc1* allele was expressed in GNPs from the normal P7 cerebellum of both wild-type and $Ink4c^{+/-}$ mice, *Ptc1* signals were not detected by quantitative real-time PCR in purified tumor cells from four of four MBs (dark-gray bars). Comparison of *Ink4c* expression in normal P7 cerebella from $Ink4c^{+/+}$ versus $Ink4c^{+/-}$ mice revealed a reduction of gene expression in the latter tissues, consistent with gene dosage (Fig. 5C, light-gray bars). However, unlike the case for *Ptc1*, *Ink4c* expression was maintained in tumor cells. (See Note Added in Proof.)

Because *p53* inactivation was required to ensure a high penetrance of MB in all previous mouse models so far studied, we used RT–PCR to amplify *p53* transcripts from tumors arising in $Ptc1^{+/-}$ mice lacking one or both *Ink4c* alleles. We then cloned 10 individual cDNAs from each tumor and determined their nucleotide sequences. Even if such transcripts were amplified from both tumor and nontumor cells, we reasoned that sequencing of multiple transcripts from each tumor would reveal mutations if they were present. In six tumors, three of each genotype, no mutations in *p53* were detected. Because mutations in p53 affect its ability to induce Mdm2, which, in turn, triggers p53 destruction (Haupt et al. 1997; Kubbutat et al. 1997), a hallmark of p53 mutation is its accumulation to relatively high levels. When sections of the same tumors were immunostained with an antibody to p53, its levels of expression were characteristically low. Irradiated tissues containing wild-type *p53* exhibited strong p53 induction, whereas those from irradiated *p53*-null mice lacked any signal (data not shown). Therefore, the increased incidence of MB following loss of *Ink4c* alleles in mice heterozygous for *Ptc1* does not require *p53* inactivation.

INK4C loss of function in human MB

In contrast to the related family member *INK4A* (*CDKN2A*), mutations or deletions of *INK4C* are rarely observed in human tumors (Ruas and Peters 1998). However, promoter methylation of *INK4C* occurs in Hodgkin

lymphoma (Sanchez-Aguilera et al. 2004) and reduced $p18^{INK4C}$ expression has been observed in several tumor types (Bartkova et al. 2000; Buchwald et al. 2004; Morishita et al. 2004). We therefore analyzed MBs for *INK4C* promoter methylation and protein expression.

In a cohort of 23 tumors studied by methylation-specific PCR, one exhibited complete *INK4C* promoter methylation and three were hemimethylated (Supplementary Fig. 3). In contrast, *INK4C* promoter methylation was not observed in nine samples of normal cerebellum or in 11 immortalized human MB cell lines. Methylation of the *INK4A* locus was not detected.

A separate cohort of 73 MB samples was analyzed by immunohistochemical staining (IHC) (Fig. 6). Tumor samples chosen to be histopathologically representative of the tumors from which they arose were incorporated into tissue microarrays, each of which had previously been stained with antibodies to ERBB2, SFRP1, GLI1, and other neuronal markers, thereby confirming their integrity for IHC analysis. MB tumor cells, readily identified by their characteristic morphology, segregated into three classes based on $p18^{INK4C}$ expression: 17 (23%, scored here as grade 2) stained strongly (Fig. 6A), 42 (58%, grade 1) showed intermediate levels (Fig. 6B), and 14 (19%, grade 0) yielded virtually no signal (Fig. 6C). As expected, all tumors stained positively in parallel analyses performed with antibodies to cyclin D1 (data not shown). Of the 73 patient samples so analyzed, 46 have been subjected to a more comprehensive analysis, including microarray gene expression profiling, a genome-wide survey for alterations in gene copy numbers, and nucleotide sequencing of candidate tumor-promoting genes. A 100K SNP array analysis did not reveal deletions in the region of the *INK4C* (*CDKN2C*) locus in any of 30 samples, and *INK4C* RNA was still expressed, implying that alterations in $p18^{INK4C}$ protein expression reflect post-transcriptional regulatory mechanisms. Of three of 46 cases that had *TP53* mutations and of seven that had mutations in the *PTC1* pathway, each expressed $p18^{INK4C}$. Six of the seven samples with *PTC1* pathway mutations scored as IHC grade 1. The number of patient samples so far analyzed precludes significant correlations with *TP53* or *PTC1* status. These data nonetheless provide the first evidence that loss of $p18^{INK4C}$ expression is a relatively frequent event in human MB.

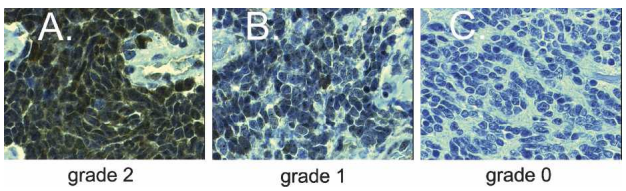

Figure 6. Immunohistochemical staining of representative human MBs with antibody to $p18^{INK4C}$. *A–C* illustrate differential staining of tumor cells scored as grade 2, grade 1, and grade 0, respectively. Tissues histopathologically representative of tumor blocks incorporated into microarrays were simultaneously stained with antibodies to other markers to confirm the integrity of the samples and identity of the tumor cells.

Discussion

The 'Rb pathway' in postnatal cerebellar development

During postnatal cerebellar development, the *Ink4c* gene is activated in GNPs within the EGL but is extinguished as post-mitotic cells migrate to form the IGL. In contrast, $p27^{Kip1}$ expression is restricted to post-mitotic neurons in the EGL and maintained in granule neurons throughout adult life. Inactivation of N-*Myc* in neuronal progenitors triggers a dramatic up-regulation of both *Ink4c* and *Kip1* in the cerebellar anlage that accompanies defective organogenesis (Knoepfler et al. 2002), so repression of these CDK inhibitors is likely required during embryonic stages of cerebellar development. Although it is well appreciated that $p27^{Kip1}$ is stabilized and accumulates in quiescent cells (Sherr and Roberts 1995), the factors that control the transient expression of *Ink4c* in the EGL remain unknown.

The only role for $p18^{Ink4c}$ is to inhibit the activity of cyclin D-dependent kinases (Sherr and Roberts 1995; Pei et al. 2004; Sotillo et al. 2005), whose proper regulation is central to cerebellar development (Ciemerych et al. 2002). Expression of $p18^{Ink4c}$ should thereby enhance the functions of the retinoblastoma family of proteins (Rb, p130, and p107) that govern both cell cycle exit and differentiation in many biological settings (Sellers et al. 1998; Morris and Dyson 2001; Müller et al. 2001; Trimarchi and Lees 2002; Classon and Harlow 2002; Thomas et al. 2003; Bracken et al. 2004; Cam et al. 2004). Rb is expressed in both developing and mature cerebellar granule cells and Purkinje neurons (Utomo et al. 1999). In contrast, p107, while readily detected during embryonic and postnatal cerebellar development, is rapidly down-regulated as GNPs terminally differentiate, and p130 is expressed at relatively low levels at all of these stages (Marino et al. 2003). Like *Ink4c*, *Rb* is nonessential for cerebellar development, but GNPs with targeted *Rb* disruption exhibit a delay in terminal differentiation and migration, and a significant fraction undergoes apoptosis within the inner EGL and IGL, a process exacerbated in GNPs lacking both *Rb* and *p107*. Disruption of the "Rb pathway", either through loss of Ink4 proteins or Rb itself, or via overexpression of cyclin D-dependent kinase activity, is a hallmark of cancer (Sherr 1996; Hanahan and Weinberg 2000). Yet, perturbations affecting the functions of these proteins have not as yet been described in human MBs.

Ink4c and p53 collaborate to suppress medulloblastoma

GNPs taken from the P7 cerebellum have a greater proliferative capacity than those harvested later when neuronal progenitors have already begun to exit the cell division cycle and migrate into the IGL. When explanted into culture in the absence of Shh, GNPs rapidly exit the cell cycle and differentiate, but Shh addition extends their proliferative potential. GNPs harvested from *Ink4c*-null and *p53*-null mice invariably demonstrated a greater proliferative advantage than their wild-type

counterparts, either in the presence or absence of Shh, and inactivation of both genes yielded additive effects. Unlike certain *p53*-null mouse cells, such as embryonic fibroblasts, astrocytes, and bone marrow-derived B-lymphocytes that retain their growth factor dependency but bypass senescence (Lowe and Sherr 2003), cultured *p53*-null GNPs differentiate and therefore exhibit a relatively limited replicative potential.

Neither *p53* nor *Ink4c* inactivation alone enables the spontaneous formation of MBs, and <25% of DKO mice develop these tumors, implying that other events are required for more rapid tumor development. The complete loss of *Ptc1* expression in some of these tumors and the up-regulation of the *Ptc1* signaling pathway in all suggest that *p53* loss might provide an environment in which *Ptc1* mutations occur at greater frequency. Irradiation of *p53*-null animals at P5, or of mice in which *p53* was conditionally inactivated in somatic cells with Nestin-Cre, induced medulloblastomas in the vast majority of animals, whereas unirradiated *p53*-null mice rarely develop these tumors (<1%). This underscores the role of the p53 checkpoint in normally eliminating cells that have sustained DNA damage during the phase of rapid proliferation that marks the expansion of the EGL. Although irradiated *Ink4c*-null mice did not develop tumors, abnormal ectopic foci of nonproliferating neuronal cells could be identified within the molecular layer of their cerebella, implying that progenitor cells within the EGL did not properly exit this compartment at earlier stages of development. Hence, inactivation of *p53* at an early stage may allow such cells to remain in cycle, thereby increasing the probability of tumor formation.

Ink4c collaborates independently with Ptc1 to suppress tumorigenesis

A bellwether finding is that *Ink4c* loss significantly accelerated MB formation in $Ptc1^{+/-}$ mice without a requirement for *p53* inactivation. This more closely mimics many human MBs that exhibit defects in the SHH signaling pathway without accompanying *TP53* mutations. Culture of GNPs from $Ink4c^{-/-}$–$Ptc1^{+/-}$ mice again revealed that combined gene loss endowed cells with an additive proliferative advantage in the absence of Shh stimulation. In agreement with this finding, uncultured MB tumor cells purified from $Ink4c^{+/-}$–$Ptc1^{+/-}$ mice exhibited an S-phase fraction that mimicked that of normal GNPs recovered from P5 cerebella, consistent with results of gene expression profiling that highlight the relationship between MBs and cells in the P5 cerebellum.

The idea that *Ptc1* is haploinsufficient for tumor suppression has remained controversial, since some investigators have reported expression of the wild-type *Ptc1* allele in tumor tissue (Wetmore et al. 2000; Zurawel et al. 2000) and others have not (Berman et al. 2002; Pazzaglia et al. 2002; Oliver et al. 2005). Using discriminating primers, we detected expression of the wild-type *Ptc1* allele in some $Ptc1^{+/-}$ tumor tissues by RT–PCR regardless of their *Ink4c* status, but we could not exclude that *Ptc1* was expressed by contaminating nontumor cells. Separation of "dense", GNP-like, *Math1*-positive tumor cells from the remaining cells in four of four medulloblastomas arising in $Ptc1^{+/-}$–$Ink4c^{+/-}$ mice, followed by reanalysis of *Ptc1* expression by quantitative real-time PCR, revealed that the wild-type *Ptc1* gene was inactivated. However, *Ink4c* continued to be expressed in these same tumor cells, consistent with a previous report that it is haploinsufficient for tumor suppression in other settings (Bai et al. 2003). Such findings underscore the difficulties in formally proving that some tumor suppressors function in a dose-dependent manner (Quon and Berns 2001; Sherr 2004).

INK4C in human MB

In marked contrast to *INK4A* (*CDKN2A*), which is frequently inactivated in many tumor types by point mutations, deletions, and gene silencing, mutations or deletions affecting the *INK4C* (*CDKN2C*) locus have only rarely been detected in human cancers (Ruas and Peters 1998). However, promoter methylation of *INK4C* occurs frequently in Hodgkin lymphomas (Sanchez-Aguilera et al. 2004), and reduced $p18^{INK4C}$ protein expression has been reported in parathyroid adenomas (Buchwald et al. 2004), poorly differentiated hepatocarcinomas (Morishita et al. 2004), and invasive germ cell tumors (Bartkova et al. 2000).

A survey of 23 MB samples revealed that the *INK4C* promoter was hemimethylated in three cases and fully methylated in one. No *INK4C* promoter methylation was detected in 11 established human medulloblastoma cell lines that lack a microarray expression signature for SHH pathway activation and, in turn, do not respond to physiologic levels of SHH antagonists. Similarly, *INK4C* methylation was not observed in normal human cerebellar tissues. Hemimethylation of the *INK4C* promoter would bear significance if the gene is haploinsufficient for tumor suppression in humans as it can be in mice. Moreover, the overall frequency of *INK4C* methylation (17%) eclipses that of *TP53* mutations.

Immunohistochemical analysis of MB samples from a larger independent cohort of 73 patients revealed an absence of detectable $p18^{INK4C}$ protein expression in 14 cases (grade 0). An equivalent number of cases exhibited very strong $p18^{INK4C}$ expression (grade 2), whereas the remainder yielded an intermediate level of IHC staining (grade 1). In contrast, representative samples subjected to 100K SNP array analysis and microarray expression profiling exhibited no loss of *INK4C* copy number or absence of gene expression. Therefore, the lack of $p18^{INK4C}$ protein expression in some MBs, and its reduced expression in others, must depend upon post-transcriptional mechanisms. These results are reminiscent of those previously obtained with *KIP1*, which is not mutated, deleted, or frequently silenced in human cancers and was therefore initially not thought to function as a tumor suppressor gene in humans. Nonetheless, *KIP1* is haploinsufficient for tumor suppression in the mouse (Fero et al. 1998), and it is now well appreciated that reduced $p27^{Kip1}$ protein expression, due to its accelerated turn-

over in tumor tissues, occurs frequently in many cancers and connotes a poor prognosis (Blain et al. 2003). As for $p18^{INK4C}$, the only manner by which $p27^{KIP1}$ levels in tumors can be quantified is by IHC analyses. This has proven highly predictive of clinical outcome in human breast, prostate, and colon cancer (Catzavelos et al. 1997; Porter et al. 1997; Thomas et al. 1998; Tsihilias et al. 1998; Alkarain and Slingerland 2004), even where tumor cells infiltrate normal epithelial glands and stroma and are therefore more difficult to score than the sheets of small, densely packed cells that characterize MBs. Without considering whether $p18^{INK4C}$ haploinsufficiency might contribute to the grade 1 MBs scored in this study, the absence of detectable $p18^{INK4C}$ protein in 19% of tumors implicates *INK4C* in their pathogenesis.

Materials and methods

Animal husbandry

Breeding and genotyping of the *Ink4c*-null, *p53*-null, and *Ink4c–p53*-double null mice were performed as previously described (Zindy et al. 2003). $Ptc1^{+/-}$ mice (Goodrich et al. 1997) were crossed with *Ink4c*-null mice (Franklin et al. 1998; Latres et al. 2000). Nestin-Cre (Knoepfler et al. 2002) and GFAP-Cre (Kwon et al. 2001) transgenes were bred onto the *Ink4c*-null background and animals then bred to appropriate strains to yield $p53^{-/FL}$ progeny. Genotyping of *Ptc1* and $p53^{FL}$ alleles was performed by PCR (Marino et al. 2000; Wetmore et al. 2000). Mice lacking *p53*, *Ink4c*, or both were irradiated using a cesium source at P5 or P6 with 4 Gy ionizing radiation. All mice were housed in an American Association of Laboratory Animal Care-accredited facility and maintained in accordance with NIH Guidelines. The Animal Care and Use Committee at St. Jude Children's Research Hospital approved all procedures.

Purification of primary cerebellar GNPs

GNPs were purified from mouse cerebella as per Hatten et al. (1998), with minor modifications. Briefly, cerebella from mice at P7–P14 were dissected away from the remaining brain. The pia mater was removed, and cerebella were treated with trypsin and triturated into a single-cell suspension. Cells were separated on a density step gradient of 35% and 60% Percoll solution (Sigma). Precursor granule neurons have the highest density of all the cell types in the cerebellum and can be separated from a less dense fraction that contains glial cells, Purkinje cells, and large interneurons. Purified GNPs were further enriched by panning on tissue culture dishes, twice successively, to remove adherent fibroblasts. Nonadherent cells were plated at a density of 6×10^5 cells/mL in eight-well Lab-Tek glass dishes (Nalge-Nuc Intl.) precoated with a poly D-lysine solution (Sigma) and Matrigel (BD Biosciences), either with or without Shh. Cells were grown in Neurobasal medium with B27 supplement, insulin, transferrin, selenium, 2 mM glutamine, and 100 U/mL penicillin/streptomycin (all from Gibco), linoleic acid-albumin, 0.45% D-glucose, and 16 µg/mL N-acetyl-cysteine (all from Sigma). The purity of GNPs was confirmed by staining with anti-GFAP (Chemicon) for glia and Class III β-tubulin (Tuj1, Babco) for neuronal precursors. More than 95% of GNPs expressed neuronal markers, as previously reported (Hatten et al. 1998). Shh was from conditioned medium from a 293 cell line that was engineered to express a secreted form of Shh (ShhN-pIND), generously provided by Dr. Philip Beachy (Johns Hopkins Medical School, Baltimore, MD).

Proliferation assays

The proliferation of GNPs was recorded after BrdU (Amersham Biosciences) pulses for 22-h intervals after plating cells in the presence or absence of Shh. Cells were fixed in 4% paraformaldehyde for 20 min, treated with 2N HCl for 30 min, and stained with an antibody to BrdU (Bu-20A). The percentage of BrdU-positive cells was determined by counting at least 500 cells per well, and total cell numbers were determined by counterstaining nuclei with DAPI (Sigma). Each experiment was repeated at least four times.

RNA isolation and Affymetrix microchip array analysis

GNPs were isolated from Percoll density gradients. Frozen tissues and tumors were collected, flash-frozen, and stored at –80°C. Total RNA was extracted using Trizol (Invitrogen) according to the manufacturer's instructions. RNA from medulloblastomas was subjected to microarray hybridization to the GeneChip Mouse Expression Set (MOE) 430A and B (Affymetrix), which contain ~39,000 transcripts. Expression signals of each gene were calculated using Affymetrix MAS version 5 software. Data analysis of signal intensity and statistical analyses were performed with GeneSpring version 7.0 software (Silicon Genetics) as described in Lee et al. (2003).

PCR analyses

Quantitative real-time PCR on RNA extracted from cerebella and purified GNPs at the indicated times was performed using a 7900HT Sequence Detection System and the TaqMan One-Step PCR MasterMix Reagents Kit (both from ABI). Oligonucleotide primers and a TaqMan probe for each gene were designed using Primer Express version 2.0 software (ABI). The primer/TaqMan probe sets for murine genes were *Ink4c*: 5′-GCGCTGCAGGTTATGAAAC-3′ (forward), 5′-TTAGCACCT CTGAGGAGAAGC-3′ (reverse), and 5′-CCTGGCAATCTCC GGATTTCCA-3′ (TaqMan probe); *Math1*: 5′-ATGCACGGGC TGAACCA-3′ (forward), 5′-TCGTTGTTGAAGGACGGGATA-3′ (reverse), and 5′-CCTTCGACCAGCTGCGCAACG-3′ (TaqMan probe); *Ptc1*: 5′-CCGCCTTCGCTCTGGAG-3′ (forward), 5′-TGAAACTTCGCTCTCAGCCAC-3′ (reverse), and 5′-AAG GGGAAGGCTACTGGCCGGAAAGCGC-3′ (TaqMan probe). The reaction was performed with 100 ng total RNA of each sample in triplicate reactions in a 50-µL volume containing 100 nM primers and 50 nM probe. Cycling conditions were 10 min at 25°C, 30 min at 48°C, and 10 min at 95°C, followed by a 40-cycle amplification for 15 sec at 95°C and 1 min at 60°C. Real-time PCR data were analyzed by using SDS version 2.0 software (ABI) and normalized to the internal 18S rRNA level (Lee et al. 2003). Methylation-specific PCR for *INK4C* was performed using primers and a protocol described in Sanchez-Aguilera et al. (2004).

Screening for mutations in tumor samples

Reverse transcription of RNA (1 µg) in 20-µL reactions was achieved with a SuperScript RTII kit (Invitrogen). Synthesized cDNA (2 µL) was used to amplify the full coding region of *p53* using Pfu polymerase (Stratagene) in a 30-µL reaction volume. Thermocycling conditions consisted of 4 min at 95°C and 20 cycles of 30 sec at 94°C, 30 sec at 52°C, and 90 sec at 72°C, followed by 15 min at 72°C. Taq polymerase (0.5 U) was added,

followed by incubation for 10 min at 72°C. Three separate reactions were carried out for each sample. After electrophoretic resolution on agarose gels, bands were cut and pooled together for purification (QIAquic, Qiagen) and 2-µL aliquots were taken for TOPO TA cloning (Invitrogen) according to the manufacturer's protocol. Positive colonies were sequenced using M13 forward and reverse sequencing primers. The primers used to amplify the entire coding region of p53 were forward 5′-GACTG GATGACTGCCATGGAG and reverse 5′-AAGTGATGGGAG CTAGCAGTTT.

Histopathology, in situ hybridization, immunofluorescence, and immunohistochemistry

Moribund and normal mice at the indicated ages were sacrificed, and tumors and cerebella from each animal were collected and fixed in 10% neutral-buffered formalin. Fixed tissues were embedded in paraffin, sectioned at 4 µm, and stained with hematoxylin and eosin (Zindy et al. 2003). Mice at designated ages received intraperitoneal injections of BrdU (5 mg/mL; 40 µL/g) 9 h before sacrifice, and tissues perfused in situ were prepared as described (Zindy et al. 1999). In situ hybridizations were performed with anti-sense probes as part of the Gensat program (http://www.stjudebgem.org/web/html/methods.php) and immunofluorescent detection of $p27^{Kip1}$, BrdU, and Ki67 was performed as described (Bertwistle et al. 2005) using antibodies from BD Transduction Laboratories, Oxford Biotechnology, and Novo Castra, respectively. IHC staining of medulloblastomas and cerebellar rests were performed as per Zindy et al. (2003), using antibodies to Ki67 (Vector Laboratories) and anti-GABA(A) receptor α6 subunit (Chemicon). Arrayed human MB tissues were simultaneously stained for $p18^{INK4C}$ (M168, 1/200 dilution, Santa Cruz), as previously employed for analysis of germ cell tumors (Bartkova et al. 2000) and for cyclin D1 (Zymed AM29).

Acknowledgments

We are indebted to Drs. Lee Rubin (Curis, Inc.) and Philip Beachy (Johns Hopkins School of Medicine) for generously providing purified sonic hedgehog (Shh) and cell lines producing the growth factor, and to Mathew Scott, Mariano Barbacid, Anton Berns, Robert Eisenman, and Suzanne Baker for providing $Ptc1^{+/-}$, *Ink4c*-null, $p53^{FL/FL}$, Nestin-Cre, and GFAP-Cre transgenic mice, respectively. We thank Mark and Virginia Valentine for performing spectral karyotyping; Guylaine Assem, Robert Jenson, and Shelly Wilkerson for expert help in animal husbandry and genotyping; Rose Mathew for preparing primary cultures and performing proliferation assays of GNPs; Dorothy Bush for assistance with immunohistochemistry; and Alfi Uziel for data management. This work was supported in part by the Children's Brain Tumor Foundation (M.F.R.), the V Foundation (R.J.G.), grant CA-096832 and Cancer Center Core Grant CA-21765 from the National Cancer Institute, and by ALSAC of St. Jude Children's Research Hospital. C.J.S. is an investigator of the Howard Hughes Medical Institute.

Note added in proof

We have now performed quantitative PCR analyses of *Ptc1* and *Ink4c* RNA expression in GNP-like tumor cells purified from 30 mouse medulloblastomas. As indicated in Figure 5C, six of six tumors from $Ptc1^{+/-}$–$Ink4c^{+/+}$ mice, 11 of 14 from $Ptc1^{+/-}$–$Ink4c^{+/-}$ mice, and 10 of 10 from $Ptc1^{+/-}$–$Ink4c^{-/-}$ mice expressed no detectable *Ptc1* mRNA. The 30 tumors expressed *Math1*, and all 20 tumors from $Ink4c^{+/+}$ and $Ink4c^{+/-}$ animals continued to express *Ink4c* mRNA. Thus, *Ink4c* is haploinsufficient for tumor suppression, whereas *Ptc1* is not.

References

Alkarain, A. and Slingerland, J. 2004. Deregulation of p27 by oncogenic signaling and its prognostic significance in breast cancer. *Breast Cancer Res.* **6:** 13–21.

Bai, F., Pei, X.H., Godfrey V.L., and Xiong, Y. 2003. Haploinsufficiency of p18(Ink4c) sensitizes mice to carcinogen-induced tumorigenesis. *Mol. Cell. Biol.* **23:** 1269–1277.

Bartkova, J., Thullberg, M., Rajpert-de Meyts, E., Skakkebaek, N.E., and Bartek, J. 2000. Cell cycle regulators in testicular cancer: Loss of $p18^{INK4C}$ marks progression from carcinoma *in situ* to invasive germ cell tumours. *Int. J. Cancer* **85:** 370–375.

Berman, D.M., Karhadkar, S.S., Hallahan, A.R., Pritchard, J.I., Eberhart, C.G., Watkins, D.N., Chen, J.K., Cooper, M.K., Taipale, J., Olson, J.M., et al. 2002. Medulloblastoma growth inhibition by hedgehog pathway blockade. *Science* **297:** 1559–1561.

Bertwistle, D., Zindy, F., Sherr, C.J., and Roussel, M.F. 2005. Monoclonal antibodies to the mouse $p19^{Arf}$ tumor suppressor protein. *Hybrid. Hybridomics* **23:** 293–300.

Blain, S.W., Scher, H.I., Codon-Cardo, C., and Koff, A. 2003. p27 as a target for cancer therapeutics. *Cancer Cell* **3:** 111–115.

Bracken, A.P., Ciro, M., Cocito, A., and Helin, K. 2004. E2F target genes: Unraveling the biology. *Trends Biochem. Sci.* **29:** 409–417.

Buchwald, P.C., Akerstrom, G., and Westin, G. 2004. Reduced p18INK4C, p21CIP1/WAF1 and p27KIP1 mRNA levels in tumours of primary and secondary hyperparathyroidism. *Clin. Endocrinol.* **60:** 389–393.

Cam, H., Balciunaite, E., Blais, A., Spektor, A., Scarpulla, R.C., Young, R., Kluger, Y., and Dynlacht, B.D. 2004. A common set of gene regulatory networks links metabolism and growth inhibition. *Mol. Cell* **16:** 399–411.

Catzavelos, C., Bhattacharya, N., Ung, Y.C., Wilson, J.A., Roncari, L., Sandhu, C., Shaw, P., Yeger, H., Morava-Plotzner, I., Kapusta, L., et al. 1997. Decreased levels of the cell cycle inhibitor p27KIP1 protein: Prognostic implications in primary breast cancer. *Nat. Med.* **3:** 227–230.

Ciemerych, M.A., Kenney, A.M., Sicinska, E., Kalaszczynska, I., Bronson, R.T., Rowitch, D.H., Gardner, H., and Sicinski, P. 2002. Development of mice expressing a single D-type cyclin. *Genes & Dev.* **16:** 3277–3289.

Classon, M. and Harlow E. 2002. The retinoblastoma tumour suppressor in development and cancer. *Nat. Rev. Cancer* **2:** 910–917.

Cunningham, J.J. and Roussel, M.F. 2001. Cyclin-dependent kinase inhibitors in the development of the central nervous system. *Cell Growth Differ.* **12:** 387–396.

Donehower, L.A., Harvey, M., Slagle, B.L., McArthur, M.J., Montgomery Jr., C.A., Butel, J.S., and Bradley, A. 1992. Mice deficient for p53 are developmentally normal but susceptible to spontaneous tumours. *Nature* **356:** 215–221.

Fero, M.L., Randel, E., Gurley, K.E., Roberts, J.M., and Kemp, C.J. 1998. The murine gene p27Kip1 is haplo-insufficient for tumor suppression. *Nature* **396:** 177–180.

Franklin, D.S., Godfrey, V.L., Lee, H., Kovalev, G.I., Schoonhoven, R., Chen-Kiang, S., Su, L., and Xiong, Y. 1998. CDK inhibitors $p18^{Ink4c}$ and $p27^{Kip1}$ mediate two separate pathways to collaboratively suppress pituitary tumorigenesis. *Genes & Dev.* **12:** 2899–2911.

Gilbertson, R.J. 2004. Medulloblastoma: Signalling a change in treatment. *Lancet Oncol.* **5:** 209–218.

Goldowitz, D. and Hamre, K. 1998. The cells and molecules that make a cerebellum. *Trends Neurosci.* **21:** 375–382.

Goodrich, L.V., Milenkovic, L., Higgins, K.M., and Scott, M.P. 1997. Altered neural cell fates and medulloblastoma in mouse patched mutants. *Science* **277:** 1109–1113.

Hanahan, D. and Weinberg, R.A. 2000. The hallmarks of cancer. *Cell* **100:** 57–70.

Hatten, M.E. 2002. New directions in neuronal migration. *Science* **297:** 1660–1663.

Hatten, M.E., Gao, W.Q., Morrison, M.E., and Mason, C.A. 1998. The cerebellum: Purification and culture of identified cell populations. In *Culturing nerve cells* (eds. G. Banker and K. Goslin), pp. 419–459. MIT Press, Cambridge, MA.

Haupt, Y., Maya, R., Kazaz, A., and Oren, M. 1997. Mdm2 promotes the rapid degradation of p53. *Nature* **387:** 296–299.

Hyodo-Taguchi, Y., Fushiki, S., Kinoshita, C., Ishikawa, Y., and Hirobe, T. 1998. Effects of low-dose X-irradiation on the development of the mouse cerebellar cortex. *J. Radiat. Res.* **39:** 11–19.

Jacks, T., Remington, L., Williams, B.O., Schmitt, E.M., Halachmi, S., Bronson, R.T., and Weinberg, R.A. 1994. Tumor spectrum analysis in p53-mutant mice. *Curr. Biol.* **4:** 1–7.

Kenney, A.M. and Rowitch, D.H. 2000. Sonic hedgehog promotes G1 cyclin expression and sustained cell cycle progression in mammalian neuronal precursors. *Mol. Cell. Biol.* **20:** 9055–9067.

Kenney, A.M., Cole, M.D., and Rowitch, D.H. 2003. N-myc upregulation by sonic hedgehog signaling promotes proliferation in developing cerebellar granule neurons. *Development* **130:** 15–28.

Kho, A.T., Zhao, Q., Cai, Z., Butte, A.J., Kim, J.Y., Pomeroy, S.L., Rowitch, D.H., and Kohane, I.S. 2004. Conserved mechanisms across development and tumorigenesis revealed by a mouse development perspective of human cancers. *Genes & Dev.* **18:** 629–640.

Kim, J.Y., Nelson, A.L., Algon, S.A., Graves, O., Sturla, L.M., Goumnerova, L.C., Rowitch, D.H., Segal, R.A., and Pomeroy, S.L. 2003. Medulloblastoma tumorigenesis diverges from cerebellar granule cell differentiation in patched heterozygous mice. *Dev. Biol.* **263:** 50–66.

Knoepfler, P.S., Cheng, P.F., and Eisenman, R.N. 2002. N-*myc* is essential during neurogenesis for the rapid expansion of progenitor cell populations and the inhibition of neuronal differentiation. *Genes & Dev.* **16:** 2699–2712.

Kubbutat, M.H., Jones, S.N., and Vousden, K.H. 1997. Regulation of p53 stability by Mdm2. *Nature* **387:** 299–303.

Kwon, C.H., Zhu, X., Zhang, J., Knoop, L.L., Tharp, R. Smeyne, R.J., Eberhart, C.G., Burger, P.C., and Baker, S.J. 2001. Pten regulates neuronal soma size: A mouse model of Lhermitte-Duclos disease. *Nat. Genet.* **29:** 404–411.

Latres, E., Malumbres, M., Sotillo, R., Martin, J., Ortega, S., Martin-Caballero, J., Flores, J.M., Cordon-Cardo, C., and Barbacid, M. 2000. Limited overlapping roles of P15(Ink4b) and P18(Ink4c) cell cycle inhibitors in proliferation and tumorigenesis. *EMBO J.* **19:** 3496–3506.

Lee, Y. and McKinnon, P.J. 2002. DNA Ligase IV suppresses medulloblastoma formation. *Cancer Res.* **62:** 6395–6399.

Lee,Y., Miller, H.L., Jensen, P., Hernan, R., Connelly, M., Wetmore, C., Zindy, F., Roussel, M.F., Curran, T., Gilbertson, R.J., et al. 2003. A molecular fingerprint for medulloblastoma. *Cancer Res.* **63:** 5428–5337.

Lowe, S.W. and Sherr, C.J. 2003. Tumor suppression by *Ink4a–Arf*: Progress and puzzles. *Curr. Opin. Genet. Dev.* **13:** 77–83.

Marino, S. 2005. Medulloblastoma: Developmental mechanisms out of control. *Trends Mol. Med.* **11:** 17–22.

Marino, S., Vooijs, M., van der Gulden, H., Jonkers, J., and Berns, A. 2000. Induction of medulloblastomas in *p53*-null mutant mice by somatic inactivation of *Rb* in the external granular layer cells of the cerebellum. *Genes & Dev.* **14:** 994–1004.

Marino, S., Hoogervoorst, D., Brandner, S., and Berns, A. 2003. Rb and p107 are required for normal cerebellar development and granule cell survival but not for Purkinje cell persistence. *Development* **10:** 3359–3368.

Miyazawa, K., Himi, T., Garcia, V., Yamagishi, H., Sato, S., and Ishizaki, Y. 2000. A role for p27/Kip1 in the control of cerebellar granule cell precursor proliferation. *J. Neurosci.* **20:** 5756–5763.

Morishita, A., Masaki, T., Yoshiji, H., Nakai, S., Ogi, T., Miyauchi, Y., Yoshida, S., Funaki, T., Uchida, N., Kita, Y., et al. 2004. Reduced expression of cell cycle regulator p18(INK4C) in human hepatocellular carcinoma. *Hepatology* **40:** 677–686.

Morris, E.J. and Dyson, N.J. 2001. Retinoblastoma protein partners. *Adv. Cancer Res.* **82:** 1–54.

Müller, H., Bracken, A.P., Vernell, R., Moroni, M.C., Christians, F., Grassilli, E., Prosperini, E., Vigo, E., Oliner, J.D., and Helin, K. 2001. E2Fs regulate the expression of genes involved in differentiation, development, proliferation, and apoptosis. *Genes & Dev.* **15:** 267–285.

Oliver, T.G., Read, T.A., Kessler, J.D., Mehmeti, A., Wells, J.F., Huynh, T.T., Lin, S.M., and Wechsler-Reya, R.J. 2005. Loss of patched and disruption of granule cell development in a pre-neoplastic stage of medulloblastoma. *Development* **132:** 2425–2439.

Pazzaglia, S., Mancuso, M., Atkinson, M.J., Tanori, M., Rebessi, S., Majo, V.D., Covelli, V., Hahn, H., and Saran, A. 2002. High incidence of medulloblastoma following X-ray-irradiation of newborn Ptc1 heterozygous mice. *Oncogene* **21:** 7580–7584.

Pei, X.H., Bai, F., Tsutsui, T., Kiyokawa, H., and Xiong, Y. 2004. Genetic evidence for functional dependency of p18Ink4c on Cdk4. *Mol. Cell. Biol.* **24:** 6653–6664.

Porter, P.L., Malone, K.E., Heagarty, P.J., Alexander, G.M., Gatti, L.A., Firpo, E.J., Daling, J.R., and Roberts, J.M. 1997. Expression of cell cycle regulators p27Kip1 and cyclin E, alone or in combination, correlate with survival in young breast cancer patients. *Nat. Med.* **3:** 222–225.

Quon, K.C. and Berns A. 2001. Haplo-insufficiency? Let me count the ways. *Genes & Dev.* **15:** 2917–2921.

Ruas, M. and Peters, G. 1998. The $p16^{INK4A}$/CDKN2A tumor suppressor and its relatives. *Biochim. Biophys. Acta-Rev. Cancer* **1378:** F115–F177.

Sanchez-Aguilera, A., Delgado, J., Camacho, F.I., Sanchez-Beato, M., Sanchez, L., Montalban, C., Fresno, M.F., Martin, C., Piris, M.A., and Garcia, J.F. 2004. Silencing of the p18INK4C gene by promoter hypermethylation in Reed-Sternberg cells in Hodgkin lymphomas. *Blood* **103:** 2351–2357.

Sellers, W.R., Novitch, B.G., Miyake, S., Heith, A., Otterson, G.A., Kaye, F.J., Lassar, A.B., and Kaelin Jr., W.G. 1998. Stable binding to E2F is not required for the retinoblastoma protein to activate transcription, promote differentiation, and suppress tumor cell growth. *Genes & Dev.* **12:** 95–106.

Sherr, C.J. 1996. Cancer cell cycles. *Science* **274:** 1672–1677.

———. 2004. Principles of tumor suppression. *Cell* **116:** 235–246.

Sherr, C.J. and Roberts, J.M. 1995. Inhibitors of mammalian G_1 cyclin-dependent kinases. *Genes & Dev.* **9:** 1149–1163.

Sotillo, R., Renner, O., Dubus, P., Ruiz-Cabello, J., Martin-Caballero, J., Barbacid, M., Carnero, A., and Malumbres, M. 2005. Cooperation between Cdk4 and p27kip1 in tumor development: A preclinical model to evaluate cell cycle inhibitors with therapeutic activity. *Cancer Res.* **65:** 3846–3852.

Thomas, G.V., Szigeti, K., Murphy, M., Draetta, G., Pagano, M., and Loda, M. 1998. Down-regulation of p27 is associated with development of colorectal adenocarcinoma metastases. *Am. J. Pathol.* **153:** 681–687.

Thomas, D.M., Yang, H.S., Alexander, K., and Hinds, P.W. 2003. Role of the retinoblastoma protein in differentiation and senescence. *Cancer Biol. Ther.* **2:** 124–130.

Tong, W.M., Ohgaki, H., Huang, H., Granier, C., Kleihues, P., and Wang, Z.Q. 2003. Null mutation of DNA strand break-binding molecule poly(ADP-ribose) polymerase causes medulloblastomas in $p53^{-/-}$ mice. *Am. J. Pathol.* **162:** 343–352.

Trimarchi, J.M. and Lees, J.A. 2002. Sibling rivalry in the E2F family. *Nat. Rev. Mol. Cell Biol.* **3:** 11–20.

Tsihilias, J., Kapusta, L.R., DeBoer, G., Marava-Plotzner, I., Zbieranowski, I., Bhattacharya, N., Catzavelos, G.C., Klotz, L.H., and Slingerland, J.M. 1998. Loss of cyclin-dependent kinase inhibitor p27KIP1 is a novel prognostic factor in localized human prostate adenocarcinomas. *Cancer Res.* **58:** 542–548.

Utomo, A.R., Nikitin, A.Y., and Lee, W.H. 1999. Temporal, spatial, and cell type-specific control of Cre-mediated DNA recombination in transgenic mice. *Nat. Biotechnol.* **17:** 1091–1096.

Wang, V.Y. and Zoghbi, H.Y. 2001. Genetic regulation of cerebellar development. *Nat. Rev. Neurosci.* **2:** 484–491.

Wechsler-Reya, R.J. and Scott, M.P. 2001. The developmental biology of brain tumors. *Annu. Rev. Neurosci.* **24:** 385–428.

Wetmore, C., Eberhart, D.E., and Curran, T. 2000. The normal *patched* allele is expressed in medulloblastomas from mice with heterozygous germ-line mutation of *patched*. *Cancer Res.* **60:** 2239–2246.

———. 2001. Loss of *p53* but not *ARF* accelerates medulloblastoma in mice heterozygous for *patched*. *Cancer Res.* **61:** 513–516.

Zhao, Q., Kho, A., Kenney, A.M., Yuk, D.I., Kohane, I., and Rowitch, D.H. 2002. Identification of genes expressed with temporal-spatial restriction to developing cerebellar neuron precursors by a functional genomic approach. *Proc. Natl. Acad. Sci.* **99:** 5704–5709.

Zindy, F., Cunningham, J.J., Sherr, C.J., Jogal, S., Smeyne, R.J., and Roussel, M.F. 1999. Postnatal neuronal proliferation in mice lacking Ink4d and Kip1 inhibitors of cyclin-dependent kinases. *Proc. Natl. Acad. Sci.* **96:** 13462–13467.

Zindy, F., Nilsson, L.M., Nguyen, L., Meunier, C., Smeyne, R.J, Rehg, J.E., Eberhart, C., Sherr, C.J., and Roussel, M.F. 2003. Hemangiosarcomas, medulloblastomas, and other tumors in *Ink4c/p53*-null mice. *Cancer Res.* **63:** 5420–5427.

Zurawel, R.H., Allen, C., Wechsler-Reya, R., Scott, M.P., and Raffel, C. 2000. Evidence that haploinsufficiency of Ptch leads to medulloblastoma in mice. *Genes Chrom. Cancer* **28:** 77–81.